

Multimodality Stacking with Blockwise missing values and application to the PIONeer biomarkers study for prediction of resistance to immunotherapy

Mohamed Boussena¹ Florence Monville²
Jacques Fieschi-Meric² Frederic Vely³ Pierre Milpied³
Julien Mazieres⁴ Maurice Perol⁵ Eric Vivier⁶
Laurent Greillier¹³ Fabrice Barlesi⁷ Sebastien Benzekry¹

¹Inria – Inserm team COMPO, COMPUTational pharmacology and clinical Oncology, Centre Inria Sophia Antipolis - Méditerranée, Centre de Recherches en Cancérologie de Marseille, Inserm U1068, CNRS UMR7258, Institut Paoli-Calmettes, Pharmacy faculty, Aix-Marseille University

²Veracyte SAS, Marseille, France

³Assistance Publique-Hôpitaux de Marseille (APHM), Marseille, France

⁴ Toulouse University Hospital, Toulouse, France

⁵Centre Leon Berard, Lyon, France

⁶Innate Pharma, Marseille, France

⁷Université Paris Saclay, Gustave Roussy, Inserm, Prédicteurs Moléculaires et nouvelles cibles en oncologie (U981), F-94805, Villejuif, France

Abstract

Integrating multimodal datasets in clinical oncology is frequently hindered by high dimensionality and blockwise missingness, where entire data sources are unavailable for specific patient subsets. Standard survival models often struggle with these gaps, leading to biased results or patient exclusion.

We introduce Multimodality Stacking with Blockwise missing values (MSB), a late-fusion framework for survival analysis that independently models modality-specific features before aggregating predictions via a cross-validated stacking meta-learner. MSB was validated on the PIONeer study (n=443 patients, 378 biomarkers across eight heterogeneous sources) to predict progression-free survival in advanced non-small cell lung cancer patients receiving immunotherapy.

MSB yielded higher predictive performance (C-index) than baseline algorithms. Improvements varied by baseline strength: linear models showed a 15.9% increase ($p < 0.001$ for the Wilcoxon signed-rank test, consistent across 15 cross-validation folds), random survival forests gained 5.4% ($p = 0.002$), and gradient boosting methods improved by 2.1% ($p = 0.030$). Beyond discrimination, MSB reduced the generalization gap (train-test difference in 5 folds cross-validation repeated 3 times: 0.055 vs 0.380 for linear models). Permutation importance analysis identified routine laboratory markers, clinical features, and PD-L1 expression as primary predictive drivers. Missing block indicators showed negligible importance, suggesting the model learned from biomarker values rather than data availability patterns.

MSB provides a statistically validated framework for multimodal survival prediction with blockwise missingness. By enabling systematic biomarker evaluation without requiring complete data, MSB offers a practical tool for predictive modeling in biomedical research, pending external validation. Implementation of the MSB framework is available here under Inria license.

1 Introduction

In many biomedical applications, three major issues frequently occur: (1) high dimensionality ($n \sim p$ or $n \ll p$), (2) a substantial proportion of missing data and (3) high multicollinearity among features within the same data source. While conventional feature selection and ensemble-based algorithms aim to mitigate the 'curse of dimensionality' [27], they exhibit significant statistical instability in small cohorts, especially among correlated predictors. This problem has been studied by Bakmach et al. [3], to address this issue in the classification setting. These issues are compounded with missing values as standard imputation techniques lose fidelity as dimensionality increases. Given that high dimensionality in clinical datasets often arises from the integration of heterogeneous data sources, we hypothesize that addressing the problem at the source level — rather than the feature level — provides a more robust framework for survival modeling.

This source-level approach aligns with an active field of machine learning: multimodal learning, which is closely connected to multi-kernel, mixture-of-experts, or multiview learning [23, 37, 20, 14]. While often applied to integrate heterogeneous data types (e.g. tabular data and images), multimodal learning gives us a structured way to handle tabular data coming from many different sources. Kroner et al. [20] identified three principal categories of multimodal learning: early fusion, intermediate fusion, and late fusion. Early fusion encompasses approaches that combine different data modalities prior to the learning step. This would correspond to a straightforward concatenation of all features from every modality into a single dataset, with or without prior transformation. This is the simplest and most commonly used approach for handling multimodal tabular data. Intermediate fusion designates methods in which fusion and learning occur simultaneously, for instance by assigning weights to modalities or by transforming the dataset during training. Late fusion, in contrast, describes approaches that first train separate models for each modality, and subsequently merge their outputs using a final model or a rule-based scheme. This taxonomy can be extended by including 'hybrid fusion' strategies [38], which refer to any fusion approach that combines aspects of the three aforementioned categories.

While multimodal integration of imaging, omics, and tabular data offers significant potential for biomarker discovery [29], clinical oncology datasets are frequently constrained by small sample sizes and high rates of missing values. Regardless of the fusion strategy considered, current multimodal approaches commonly address blockwise missingness through listwise deletion — the exclusion of patients lacking complete data across all modalities [19, 10]. Beyond the substantial reduction in effective sample size this entails, such exclusions are rarely justified by the underlying missingness mechanism and have been shown to introduce systematic bias in predictive models [9].

Missing values in multimodal learning are receiving attention, especially for deep learning models [35]. For smaller sample sizes, Shuo Xiang et al [36] proposed a model based on late fusion where they trained an intermediate model for each modality, when available, and then imputed the missing scores. Then, a

meta model was trained on top of this reduced dataset. Van Loon et al. [22] went further with the proposal of a Stacked penalized logistic regression (StaPLR) as an imputation model to overcome missing modalities in a multimodal dataset. StaPLR fits an intermediate model on each modality, performing feature selection at the modality level, and then imputing the data, for classification tasks. The HealNet model [17] was introduced for survival analysis and is capable of dealing with missing data at the modality level. However, it is a deep learning model primarily designed for imaging data and treats tabular variables on a per-feature basis rather than as a unified modality.

Here, we departed from a nationwide clinical dataset collected to address a current problem in immuno-oncology: to predict the onset of resistance to immune-checkpoint inhibitors (ICI) in advanced non-small cell lung cancer (NSCLC). Indeed, long-term remissions are only achieved in 20-30% of such patients [5, 13, 12], making lung cancer the leading cause of cancer-related deaths [6]. A French national consortium grouping 17 clinical centers and 6 biological and industrial partners was constituted within the PIONeeR (Precision Immuno-Oncology for advanced Non-Small Cell Lung Cancer Patients with PD1(L1) ICI Resistance) clinical study (2018-2024) [4]. The biological markers from either the peripheral blood or tumor tissue collected pre-treatment yielded a dataset with 378 biomarkers in 443 patients. Because each partner processed samples to generate specific biomarker types, the data exhibited both a multi-modal structure and blockwise missing values. Although the primary endpoint was primary resistance, defined either for monotherapy as having a best overall response (BOR) of Progressive Disease or Stable Disease at 6 months, or for combination therapy – chemotherapy plus immunotherapy – as having disease progression within 6 months, even when the BOR is Complete Response or Partial Response, [26, 30], the study revealed that progression-free survival served as a more relevant continuous endpoint, prompting us to adopt here survival analysis methods.

We developed a multimodal approach relying on a stacking algorithm as an aggregating learner from multiple sources [34, 21]. While late-fusion strategies have been explored for classification [8], their extension to right-censored survival data remains under-researched. In the scikit-survival library [25], the stacking procedure merges model outputs without applying cross-validation during aggregation, which exacerbates overfitting and leads to poor performances in external sets. MSB decouples modality-specific learning from global aggregation, training independent base-learners on available data sources before merging their outputs via a cross-validated stacking meta-learner. This architecture provides a dual advantage: it mitigates the "curse of dimensionality" by reducing the input space of the final aggregator and handles blockwise gaps by aggregating risk scores rather than raw features.

2 Methods

2.1 Motivation: the PIONeeR RHU biomarkers dataset

The PIONeeR RHU (University Hospital Research) project is a nationwide multi-center prospective that screened patients suffering from advanced NSCLC treated with inhibitors of the programmed-death 1 (PD1) - programmed-death ligand 1 (PDL1) axis (NCT03493581). The study was approved by the French ethics committee (Comité de Protection des Personnes Ouest II Angers, no. 2018/08) and the French drug and device regulation agency (Agence Nationale de Sécurité du Médicament, no. 2018020500208). Informed consent was obtained from each participant before any study procedure. The samples originated from biopsies, blood samples, and clinical examinations, at multiple times prior- and on-treatment. We focus here on the former ones, consisting in a total of 378 biomarkers. The aim of the study was to provide a better understanding of resistance to anti-PD1 therapy. The project involved 17 hospitals across the country. After exclusion criteria, there remained 443 patients available for analysis.

The data collection was organized in two steps (summarized in Figure S1). The samples were first collected at each clinical center and then distributed to several platforms for specific analyses, creating the multiple (8) sources of this study. The first source consisted of clinical data (source A). These are routinely recorded variables at the time patients were registered and include age, gender, and initial characteristics of the patients' disease (e.g., histology). The second source, medical biology (source B), was also compiled independently at each medical center. It reflects the patient's biological status more directly, as it is based on biomarkers from, e.g., blood counts or biochemistry. This information is routinely collected during patient care. More advanced circulating biomarkers originated from blood samples processed at two specialized sites: Immuno-monitoring at the immuno-profiling platform Marseille Immunopôle (or MIIPP, source C), located at the Marseille University Hospital (APHM), and vascular monitoring at the vasculomonitoring platform (or MIVBL, source D), also at APHM.

Tumor tissue samples were analyzed across three laboratories. The pathology department of APHM performed standard ImmunoHistoChemistry(IHC) analyses, including, e.g., programmed-death ligand 1 (PDL1) staining (source E). These data were divided into two sources: one for PDL1 expression and another for mutations (source F) detected in tumor tissue (complemented by whole-exome sequencing performed by Veracyte). In addition, multiplex IHC staining was performed by Veracyte (formerly HaliuDx, source G) to quantify infiltration of several (sub-)populations of immune cells, and multiplex immunofluorescence staining was carried out by InnatePharma (source H). All these sources, along with the rationale for this broad and in-depth profiling, are described in details in Barlesi et al. [4].

Regarding the outcome, we focused here on Progression Free survival (PFS), defined by either death of the patient or progression of the disease according

to the RECIST criterion (Response Evaluation Criteria in Solid Tumors), a standard evaluation criterion for solid tumors [11]. We also produced results on progression only as a potential outcome, ie using only RECIST evaluation (summarized results in appendix).

2.2 Multimodality Stacking with Blockwise missing values (MSB)

The primary contribution of this work is the MSB algorithm, a meta-learning framework designed to address three concurrent challenges in clinical survival analysis: high-dimensionality, missing data and multicollinearity. It follows a late fusion paradigm, with an aggregation step explicitly accounting for the missingness pattern. It is implemented in a stacking framework . To handle these challenges, we propose to leverage the observed blockwise missingness patterns of the data.

To do so, we propose three strategies. The first, straightforward, consists of imputing the original data before splitting it into modalities (MSB_{imp} , Figure 1). The second, analogous to the approach of van Loon et al. [22], performs imputation on source-aggregated survival risk scores (e.g., hazards, see below), before a stacking step (MSB). In these two strategies, we used a kNN (k Nearest-Neighbour) imputer with default parameters, to limit computation time while preserving predictive stability [31]. The third strategy applies missing incorporated in attributes (MIA) directly within the meta-learner instead of using imputation (MSB_{MIA} , [32]). In this approach, the missingness itself is treated as an additional category and is included in the splitting rules of the tree-based model, without replacing the missing values (Figure S2). This choice was guided by the review of Josse et al. [18], which recommends MIA as suitable regardless of the underlying missingness mechanism. In our setting, this method was used when the meta-learner was a Random Survival Forest.

Our proposed approach aggregates predictions of three models within each modality: a penalized Cox model, a random survival forest model, and a component-wise boosting survival model [7]. The base learners are first fitted on all patients of the training dataset on the modality’s features. The "meta-learner" is then trained using the out-of-fold cross-validated predictions (risk scores) from these base estimators, to mitigate the risk of overfitting. This hierarchical approach reduces the input space of the final aggregator to a parsimonious set of modality-specific risk scores. We added with the computed risk scores the block missingness rate as it has been showed that adding the mask in benchmarking missing values increases performance[24] and to control whether the algorithm is learning from missingness pattern or biomarkers value.

To ensure complete input for base learners, we applied source-specific kNN imputation: if a source contained residual missingness after accounting for blockwise patterns, a kNN imputer (with default hyperparameter) was fitted and applied independently within that source. This two-stage approach distinguishes between structural blockwise missingness (entire sources absent for patient subsets, handled by MSB’s aggregation architecture) and residual feature-level gaps

(handled by local imputation).

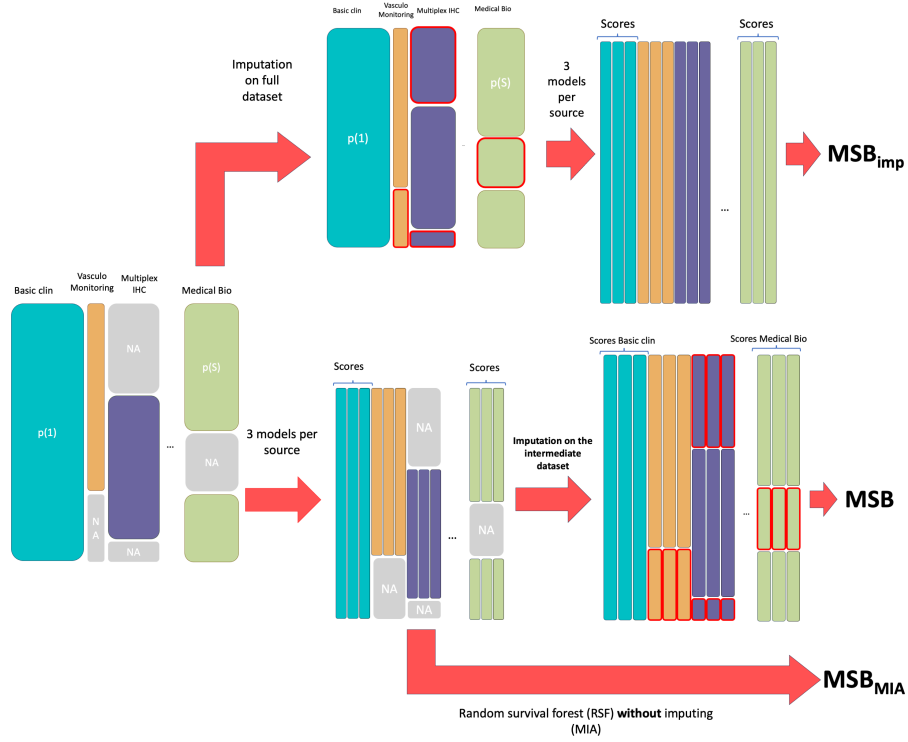


Figure 1: Multimodality Stacking with Blockwise missing values

The MSB algorithm is formalized as follows. The complete features matrix is denoted by X . We denote by $n(s)$ and $p(s)$ the number of rows and columns, respectively, for the data source $s \in \{1, \dots, S\}$. NA denotes the missing value indicator. $[X_s | X_r]$ is the concatenation operation, an outer jointure on the indexes, meaning that indices present in X_s but not in X_r are filled with missing values in source r , and respectively for X_r . The algorithm is split in two: the first specifies training (Algorithm 1), the second predictions (Algorithm 2).

Algorithm 1 Multimodality Stacking with Blockwise missing values algorithm:
Training

Require: S sources of data,
 n total number of rows,
 $X_s \in \mathbb{R}^{n(s) \times p(s)}$ for $s \in [1, S]$,
 $y \in \mathbb{R}^{n \times 2}$, \triangleright time-to-event variable and censoring indicator
 $X = [X_1 | \dots | X_S] \in (\mathbb{R} \cup \{\text{NA}\})^{n \times \sum_{s=1}^S p(s)}$
 $\mathcal{M}_1, \dots, \mathcal{M}_M$ models
 \mathcal{ML} the meta-learner
Type of MSB : between 'imp', 'MIA' and ' ' Missingness Indicator : True or False
 $R_1 \dots R_S$ The rate of missingness per block

Ensure: $\hat{Z} \leftarrow$ Empty dataset with n rows

if 'imp' **then**
 $X \leftarrow$ Fitting an imputer and imputing X

else if **then**
No Imputation

end if

for s in $1:S$ **do**
if if intra-source missingness exists in X_s
Fit kNN imputer and impute X_s 's missing values **then**
end if
 $cv \leftarrow$ cross validation on X_s
for m in $1, \dots, M$ **do**
 $\widehat{\mathcal{M}}_{m,s,cv} \leftarrow$ Fit model \mathcal{M}_m on in-folds of X_s 's cv
 $\hat{Z}_{m,s} \leftarrow$ out of fold predictions of $\widehat{\mathcal{M}}_{m,s,cv}$ concatenated by row
end for
 $\hat{Z} \leftarrow [\hat{Z} | \hat{Z}_{1,s} | \dots | \hat{Z}_{M,s}]$
for m in $1, \dots, M$ **do**
 $\widehat{\mathcal{M}}_{m,s} \leftarrow$ Fit model \mathcal{M}_m on X_s
end for
end for

if 'MIA' **then**
No Imputation on \hat{Z}

else if **then**
 $\hat{Z} \leftarrow$ Fitting an imputer and imputing \hat{Z}

end if

if Missingness Indicator **then**
 $\hat{Z} \leftarrow [\hat{Z} | R_1 | \dots | R_S]$

end if $\widehat{\mathcal{ML}} \leftarrow$ Fit \mathcal{ML} on \hat{Z}

return $\widehat{\mathcal{ML}}, \{\widehat{\mathcal{M}}_{m,s}, m \in [1, M], s \in [1, S]\}$

For a new set of features X_{new} , the prediction is the one of $\widehat{\mathcal{ML}}$ on the predictions of each $M \times S$ fitted models (each $\widehat{\mathcal{M}}_{m,s}$) on X_{new} .

Algorithm 2 Multimodality Stacking with Blockwise missing values algorithm: Predictions

Require: S sources of data,
 n total number of rows,
 $X_s \in \mathbb{R}^{n(s) \times p(s)}$ for $s \in [1, S]$,
 $X = [X_1 | \dots | X_S] \in (\mathbb{R} \cup \{\text{NA}\})^{n \times \sum_{s=1}^S p(s)}$
 $\{\widehat{\mathcal{M}}_{m,s}, m \in [1, M], s \in [1, S]\}$ Fitted models,
 $\widehat{\mathcal{M}}\mathcal{L}$ a fitted meta-learner
Missingness Indicator : True or False
 $R_1 \dots R_S$ The rate of missingness per block

if ‘imp’ **then**
 $X \leftarrow$ impute X with fitted imputer
else if **then**
No Imputation
end if

for s in 1: S **do**
if if intra-source missingness exists in X_s **then**
Impute X_s ’s missing values on saved source specific kNN imputer
end if
for m in 1: M **do**
 $Z_{m,s} \leftarrow \widehat{\mathcal{M}}_{m,s}(X_s)$
end for
 $\hat{Z} \leftarrow [\hat{Z} | \hat{Z}_{1,s} | \dots | \hat{Z}_{M,s}]$
end for

if ‘MIA’ **then**
No Imputation on \hat{Z}
else if Missingness Indicator **then**
 $\hat{Z} \leftarrow [\hat{Z} | R_1 | \dots | R_S]$
end if
 $\hat{Z} \leftarrow$ imputing \hat{Z} with fitted imputer
return $\widehat{\mathcal{M}}\mathcal{L}(\hat{Z})$

MIA (missing incorporated in attributes) is represented in Figure S2.

2.3 Metrics

The performance of each models was assessed using three repetitions of a 5-fold cross-validation procedure, stratified by length of survival (using a discretized variable), censoring and line of patients. This strategy provides a more reliable estimate of performance while keeping computational cost reasonable. For each fold, training was performed with algorithm 1 and predictions with 2. We used scikit-survival [25] together with the scikit-learn API [8].

To assess whether MSB’s improvements were statistically significant rather than attributable to random variation across cross-validation folds, we conducted paired Wilcoxon signed-rank tests comparing each MSB variant to its

corresponding baseline. Wilcoxon tests were chosen over parametric t-tests due to the bounded nature of C-index values. All p-values were corrected for False Discovery Rate (FDR) using the Benjamini-Hochberg procedure to control for multiple comparisons.

Performance

To compare the algorithms, we used the C-index and the integrated Brier Score (iBS) ([16, 15]). The purpose was to compare algorithms both at ranking risk (C-index) and at predicting true survival (iBS). When examining the iBS scores, we aimed to determine whether MSB algorithms performed better in the short term (to see which algorithm could differentiate best the early progressors from the others) or/and in the long term. Therefore, two iBS were calculated: 1) from day 15 to day 102 and 2) from day 100 until day 1000 in the results section, namely ‘iBS Early’ and ‘iBS Late’. The lower bound of the short-term window was defined by the earliest observed event times in the training cohort, ensuring stable estimates of the baseline survivor function.

Modality importance

We also investigated the behavior of each algorithm at the modality level. To do so, we used permutation importance [2] as a way to measure the modality impact of a couple (source, trained intermediate algorithm). The metric used for permutation importance was based on the iBS but for readability we adjusted it so that ‘the higher the better’, ideally ranging from 0 to 1 (an integrated Brier score can be worse than random and therefore being above 0.25). We thus defined:

$$iBSS = 1 - \frac{iBS}{0.25},$$

inspired by the Brier Skill Score, representing the level of improvement of a Brier score compared to a reference (here 0.25, the iBS obtained from random decision).

Using this metric, permutation importance for a modality-specific risk score indexed by source s and base model m was defined as :

$$perm_{(s,m)} = iBSS_{s,m} - \frac{1}{K} \sum_{k=1}^K iBSS_{k,(s,m)}$$

where $iBSS_{(s,m)}$ is the baseline performance using the original risk score from source s and model m , and $iBSS_{k,(s,m)}$ is the performance after the k -th random permutation of that risk score. Since we are interested in modality importance, the permutation importance was measured on the intermediate scores given by the models trained on the different sources. In our case this means that we measure modality importances by calculating the permutation importances of the 3 risk scores obtained from the trained models on each 8 sources on $K = 20$ permutations.

3 Results

3.1 Missing value patterns in PIONeeR

The PIONeeR dataset comprises 378 variables for 443 observed patients. The collaborative work of the project partners (Figure S1), while providing information allowing for a deep exploration to explain the progression of the disease, also generated missing data (39%, Figure 2a). The latter could be explained by two main causes. The first is logistical: some samples were not planned to be extracted for some patients (e.g., patients from a specific clinical center). The second was due to the patients' sample availability when the analysis was conducted.

Sorting the aggregated data by source revealed that the missingness mechanism was mostly at the modality level ('blockwise missingness', Figure 2b). There was a distinct missingness mechanism for each source but at the source level, each feature seemed to share the same or almost the same missingness mechanism as other features from the same source. However, some variables also exhibited intra-block missingness—individual gaps within an otherwise available modality.

Overview of the PIONeer dataset

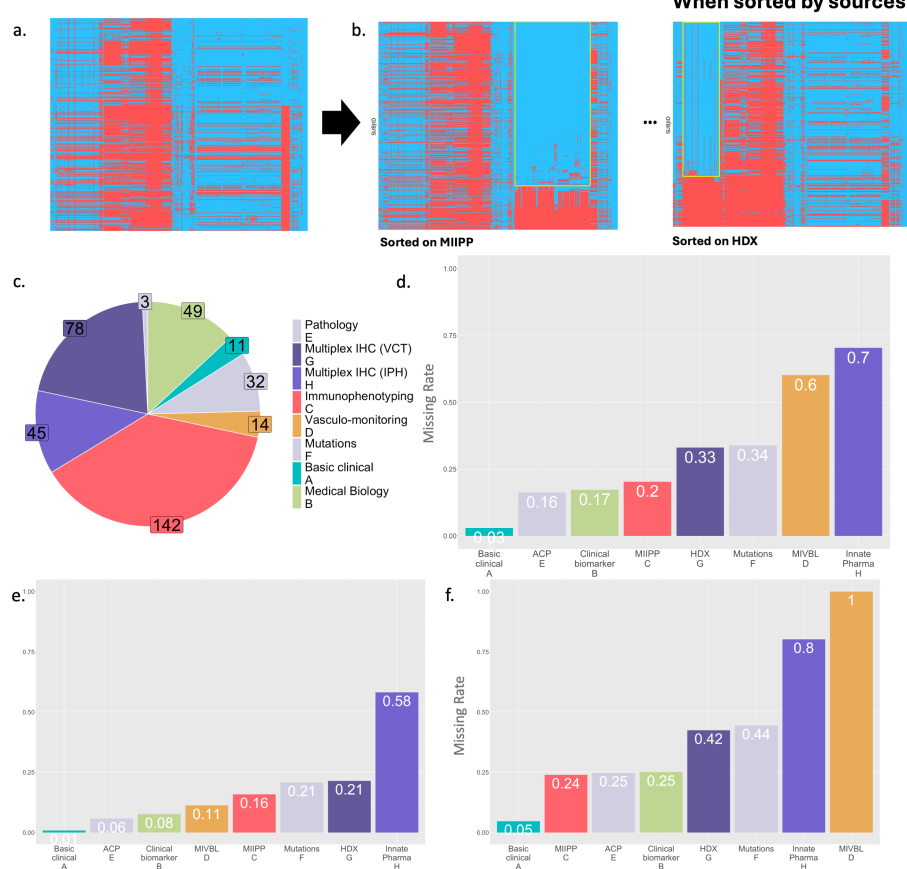


Figure 2: Multiple sources at baseline :

To visualize these patterns, we sorted the data using a binary indicator based on a 50% missingness threshold per source. This arrangement highlights the blockwise missingness structure, where specific patient cohorts are associated with the presence or absence of entire data modalities. a: General overview of missingness in the Pioneer dataset, b: Example of blockwise missingness in the Pioneer dataset when sorted by sources, the data is blue when available and red when missing, c: Number of features per sources, d: Rates of missing values' sources on full data, e: Rates of missing values' sources on APHM patients , f: Rates of missing values' sources from other centers

The number of features and missingness rates varied significantly across sources respectively from 3 to 142 features and from 3% (basic clinical) to 70% missing rate (Figure 2c & d). Basic clinical data (Source A) comprised demographics, tobacco history, and tumor characteristics (e.g., histology and number of metastases) collected during the screening visit. These features were nearly

complete ($< 5\%$ missingness), reflecting their role in routine clinical care. A critical variable in this modality was the treatment line: first-line patients received a combination of chemotherapy and ICI, whereas subsequent-line patients were treated with ICI monotherapy. As Source A integrates a broad range of general characteristics, it represents the most heterogeneous – yet most readily available – data modality in the cohort.

Among the blood-derived modalities (Sources B, C, and D), missingness rates varied significantly due to logistical stratification. While clinical biochemistry and inflammatory markers (Sources B and C) were largely available across the cohort, vasculo-monitoring (Source D) was exclusively implemented at the coordinating center (APHM), which accounted for 45% of the total cohort (Figure 2e). Consequently, this source was structurally absent for patients enrolled across the other 16 participating centers (Figure 2f). To assess whether this center-specific data availability introduced a prognostic bias, we compared Kaplan-Meier survival curves between APMH and non-APMH patients (Figure S3). The absence of a statistically significant difference between the two curves indicated that the two patient subgroups had comparable baseline survival outcomes and that MSB’s predictions were unlikely to be confounded by center identity.

To account for distinct data generation processes, we separated the data derived from pathology samples into Source E (PD-L1 expression) and Source F (mutations). This was justified by their disparate missingness rates (16% vs. 34%), which reflected the difference between standard immunohistochemistry and complex genomic sequencing.

Eventually, the tumor-derived modalities exhibited the highest rates of missingness. This sparsity was inherent to the complexity of the PIONeER protocol [4], which required up to 22 histological slides per patient to facilitate comprehensive multi-omic and pathological profiling. Missingness in these sources primarily stemmed from two factors: first, tissue exhaustion or insufficient sample quality, where specific assessments were aborted following initial pathology review; and second, logistical constraints inherent to the handling of extensive slide sets. Consequently, feature availability in these sources was directly proportional to the quantity and quality of the biopsied material.

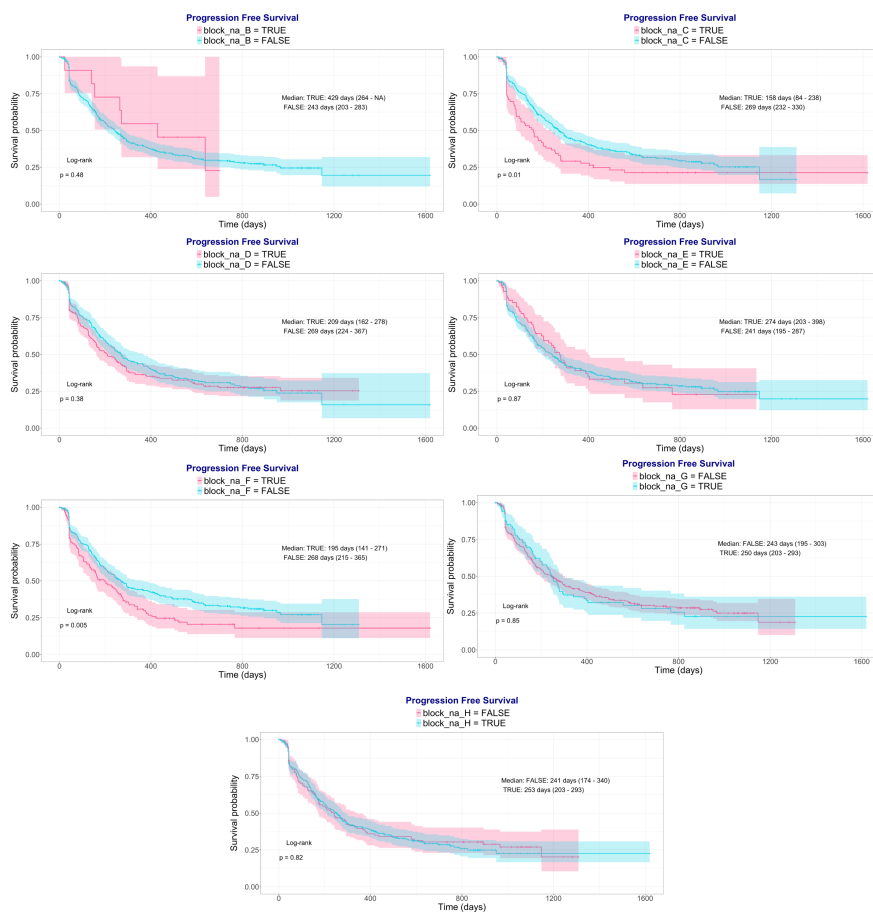


Figure 3: Kaplan-Meier curves stratified by source-level missingness. Patients were grouped by presence ($\geq 50\%$ complete) vs. absence ($< 50\%$ complete) of each data source. Source A is not shown as it exhibited $< 5\%$ missingness. Log-rank p-values are unadjusted for multiple comparisons. Two sources showed nominally significant associations: Source C (immunophenotyping, $p=0.01$) and Source F (mutations, $p=0.005$)

To assess whether blockwise missingness was associated to patient prognosis, we generated Kaplan-Meier survival curves stratified by missingness status for each data source (Figure 3). Source A was excluded from this analysis because it had almost complete data ($< 5\%$ missingness). For most sources (B, D, E, G, H), log-rank tests indicated no significant survival differences between patients with and without available data (all $p > 0.05$). However, two sources showed nominally significant associations: Source C (immunophenotyping, $p = 0.01$) and Source F (mutations, $p = 0.005$). To determine whether these associations represented independent prognostic effects or confounding by treatment line, we

repeated the analyses separately within each treatment line cohort(Figure S4). Within treatment line strata, the survival differences associated with Source C and F missingness were no longer statistically significant (all $p > 0.05$), indicating that treatment line accounted for the observed associations in unadjusted analyses.

3.2 Enhanced PFS Prediction via MSB

We configured MSB to process each of the eight data sources independently. As a result, the meta-learner was trained on a consolidated matrix of 32 input features (8 modalities \times (3 base models+block missingness rate)). This reduced feature space was intentionally chosen to ensure the model remained parsimonious, providing a stable ratio of observations to predictors for the aggregating learner. To assess the effectiveness of the MSB framework, we compared its performance with baseline survival models trained on the kNN-imputed feature set (Figure 1). Each source’s missingness rate were added as features, ensuring that the models were evaluated on the same set of features than MSB. Across all architectures — including CoxNet, Component-Wise Gradient Boosting (CWXGB), Random Survival Forest (RSF), and Gradient Boosting (XGB) — MSB consistently demonstrated superior discriminative power (Tables 1 and 2).

To facilitate a direct comparison, MSB was also evaluated on this imputed dataset (denoted by the label ‘imp’). The ‘imp’ version of MSB maintained its hierarchical structure, learning modality-specific representations separately prior to meta-aggregation. The performance of MSB remained consistent whether trained on the original sparse modalities or the imputed data. This suggests that, for this cohort, the primary challenge lies in managing high dimensionality rather than missingness alone. By decomposing the global feature space into modality-specific sub-problems, MSB effectively mitigated the complexity of the PIONeeR dataset’s heterogeneous sources.

These results indicate that for multimodal clinical data characterized by structural sparsity and high dimensionality, a structured late-fusion approach offers a more robust integration mechanism than standard unified models.

Table 1: Performance Table (5-fold CV, 3 repetitions). Bold indicates family best; * indicates global best (Test only). All models include missing block indicators. CWXGB = Component-Wise Gradient Boosting, RSF = Random Survival Forest, XGB = Gradient Boosting, MSB = Multimodality Stacking with Blockwise missing values model.

Model Family	Model	Dataset	C-index (\pm SD)	iBS Early	iBS Late
Linear	MSB-CoxNet _{imp}	test	0.663 \pm 0.030	0.123 \pm 0.011	0.225 \pm 0.036
		train	0.917 \pm 0.007	0.089 \pm 0.011	0.079 \pm 0.006
	MSB-CoxNet	test	0.658 \pm 0.034	0.117 \pm 0.007	0.223 \pm 0.033
		train	0.901 \pm 0.011	0.081 \pm 0.006	0.090 \pm 0.008
	CoxNet _{imp}	test	0.572 \pm 0.052	0.226 \pm 0.029	0.362 \pm 0.052
		train	0.952 \pm 0.007	0.024 \pm 0.003	0.039 \pm 0.006
Forest	MSB-RSF _{MIA}	test	0.682 \pm 0.028	0.106 \pm 0.005	0.192 \pm 0.019
		train	0.839 \pm 0.018	0.071 \pm 0.003	0.127 \pm 0.011
	MSB-RSF	test	0.681 \pm 0.035	0.105 \pm 0.006*	0.195 \pm 0.024
		train	0.848 \pm 0.012	0.071 \pm 0.003	0.131 \pm 0.010
	MSB-RSF _{imp}	test	0.676 \pm 0.034	0.106 \pm 0.007	0.199 \pm 0.023
		train	0.849 \pm 0.016	0.069 \pm 0.003	0.135 \pm 0.010
	RSF _{imp}	test	0.647 \pm 0.038	0.110 \pm 0.006	0.204 \pm 0.020
		train	0.932 \pm 0.004	0.044 \pm 0.001	0.054 \pm 0.001
Boosting	MSB-CWXGB	test	0.692 \pm 0.032*	0.106 \pm 0.007	0.191 \pm 0.019*
		train	0.747 \pm 0.016	0.099 \pm 0.004	0.166 \pm 0.007
	MSB-CWXGB _{imp}	test	0.687 \pm 0.039	0.106 \pm 0.007	0.194 \pm 0.024
		train	0.743 \pm 0.016	0.099 \pm 0.003	0.167 \pm 0.007
	CWXGB _{imp}	test	0.678 \pm 0.038	0.111 \pm 0.006	0.197 \pm 0.023
		train	0.741 \pm 0.008	0.105 \pm 0.002	0.173 \pm 0.005
	MSB-XGB	test	0.672 \pm 0.024	0.108 \pm 0.011	0.214 \pm 0.026
		train	0.805 \pm 0.033	0.081 \pm 0.006	0.151 \pm 0.023
	MSB-XGB _{imp}	test	0.663 \pm 0.033	0.114 \pm 0.011	0.218 \pm 0.029
		train	0.823 \pm 0.035	0.077 \pm 0.006	0.144 \pm 0.022
	XGB _{imp}	test	0.662 \pm 0.040	0.110 \pm 0.009	0.223 \pm 0.033
		train	0.938 \pm 0.005	0.051 \pm 0.002	0.069 \pm 0.003
Stacking	ScikitSurvStack	test	0.586 \pm 0.049	0.187 \pm 0.019	0.314 \pm 0.044
		train	0.928 \pm 0.008	0.036 \pm 0.002	0.057 \pm 0.005

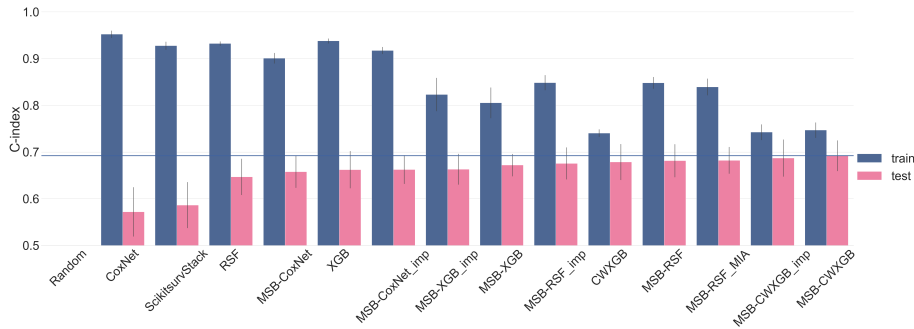


Figure 4: Summary of the results from 1 for C-index obtained sorted by their test values. This figure summarizes the table how well MSB reduces overfitting and improves performances. The line displayed is the highest mean C-index achieved on test on PFs as outcome.

Table 2: MSB framework validation: paired comparisons of MSB variants against their corresponding baseline algorithms using Wilcoxon signed-rank tests across 15 cross-validation folds (test sets only). Wilcoxon tests were chosen over t-tests due to the bounded nature of C-index values. P-values are FDR-corrected for multiple comparisons.

Base Algorithm	Δ C-index	W-stat	p-value	Adj. p
MSB-Coxnet vs CoxNet	+0.091 (+15.9%)	0	<0.001	<0.001***
MSB-RSF _{MIA} vs RSF	+0.035 (+5.4%)	7	0.001	0.002**
MSB-CWXGB vs CWXGB	+0.014 (+2.1%)	22	0.030	0.030*

* $p < 0.05$, ** $p < 0.01$, *** $p < 0.001$ (FDR-corrected using Benjamini-Hochberg method)

W-statistic: sum of ranks where baseline > MSB; lower values indicate more consistent MSB superiority

The results of tables 1 above can be summarized graphically as shown in figure 4.

3.2.1 Statistical validation of the MSB Framework

MSB significantly outperformed all baseline algorithms (all adjusted $p \leq 0.030$, (Table 2)), confirming that observed improvements were systematic rather than spurious despite the high variance inherent to small sample sizes ($n=443$). The magnitude of improvement was inversely proportional to baseline performance, demonstrating that MSB’s modality-level decomposition provides greatest value when base learners struggle with high-dimensional heterogeneous data.

The most significant improvement was observed for linear models (Table 2). MSB-CoxNet_{imp} achieved a mean C-index of 0.663 compared to standalone CoxNet’s 0.572, representing a +15.9% improvement (Wilcoxon $W=0$, adjusted $p < 0.001$). The W-statistic of 0 indicates perfect consistency: MSB-CoxNet

outperformed CoxNet in all 15 cross-validation folds without exception, demonstrating robust rather than sporadic benefit. More importantly, MSB addressed the poor calibration of the baseline linear model; the short-term iBS improved from 0.226 to 0.123, while the long-term iBS dropped from 0.362 (indicating performance worse than a random null model) to a clinically relevant 0.225.

For random survival forests, MSB-RSF achieved substantial improvement over the baseline (+5.4%, adjusted $p=0.002$, $W=7$), raising the C-index from 0.647 to 0.682. This demonstrates that even for non-linear ensemble methods, MSB’s source-level decomposition captures complementary signals that unified random forests when confronted with correlated predictors within data sources.

In contrast, component-wise gradient boosting already demonstrated strong baseline performance (C-index: 0.678), highlighting boosting’s inherent ability to handle high-dimensional, non-linear relationships through implicit feature selection. Nevertheless, MSB-CWXGB provided significant additional gains (+2.1%, adjusted $p=0.030$, $W=22$), improving the C-index to 0.692. While the improvement was more modest than for weaker baselines, the significance of the W-statistic of 22 indicates that the benefit remained consistent rather than fold-dependent. This suggests that MSB’s hierarchical structure—training modality-specific base learners before meta-aggregation—captures complementary signals that unified boosting misses, even when the unified approach already incorporates sophisticated regularization.

The pattern of differential benefit has important implications: practitioners can expect MSB to provide substantial improvements (5-16%) when applying weaker base algorithms but should still observe modest yet statistically significant gains (2-3%) even with state-of-the-art methods. Critically, the statistical validation confirms these improvements are not artifacts of high variance in small samples but represent genuine architectural advantages of the MSB framework.

3.2.2 Calibration and generalization

A consistent finding across all comparisons was that MSB not only improved patient stratification but also produced more accurate survival probabilities. The integrated Brier Scores (iBS) for both short-term and long-term windows were generally lower for models integrated with MSB compared to their standalone counterparts (Table1). This suggests that the late-fusion approach effectively leverages modality-specific signals to refine the predicted survival curves. Consistent patterns were also observed in the progression-only endpoint analysis (TableS4), though iBS values were slightly higher than in PFS, suggesting that the joint consideration of progression and death provides a richer predictive signal.

Our results indicate that all three strategies (MSB_{imp}, MSB, MSB_{MIA}) yielded comparable performances within base algorithm families (Δ C-index <0.01 , Table 1). Given this equivalence, imputing on the lower-dimensional risk scores (MSB) or using MIA may be computationally preferable for large-scale clinical applications, as these approaches avoid high-dimensional imputation on the original feature space.

Finally, a critical advantage of the MSB framework is the significant reduction in the generalization gap (the disparity between training and test performance). By acting as a regularizer through the stacking of modality-specific learners, MSB mitigated the overfitting observed in standalone models, particularly CoxNet (train-test gap: 0.380) and RSF (gap: 0.285). The gap was substantially smaller (0.055) for MSB-CWXGB. This reduction in overfitting is a prerequisite for reliable clinical deployment, as it indicates the model has learned generalizable patterns rather than dataset-specific artifacts. Among the various meta-learners tested (CoxNet, RSF, XGB, CWXGB), component-wise boosting emerged as the optimal choice for the stacking layer, consistently outperforming RSF and XGBoost in aggregating the eight modality-specific scores.

3.3 Modality importance

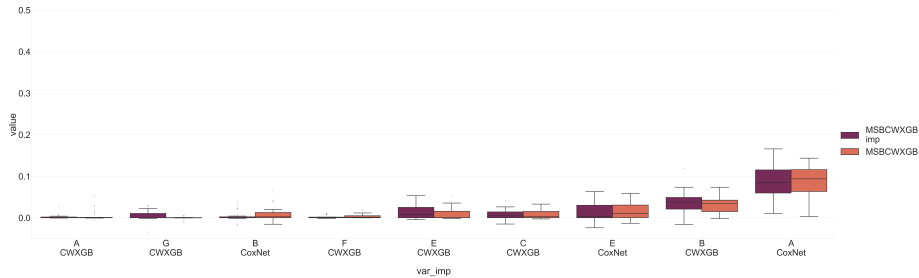


Figure 5: Top Permutation importance on iBSS for ComponentWise boosting as meta model in MSB. Each x-axis label corresponds to the couple (source, name) of the model trained on the source. The y-axis corresponds to the permutation importance value as described in the Methods section.

Model	Max importance	Max SD
MSB-CWXGB	0.001	0.003
MSB-CWXGB _{imp}	$< 10^{-3}$	$< 10^{-3}$

Table 3: Block missingness indicator importance (permutation, iBSS). Only maximum absolute value across the 8 sources reported. Near-zero values confirmed MSB learns from biomarker signal, not data availability patterns.

To clarify how decisions were made within the MSB framework, we computed the permutation importance of each modality at the meta-learner level (see Methods). Because each modality was encoded by three base-learner outputs (CoxNet, RSF, and CWXGB), importance was computed for each learner at the modality level to determine which data sources primarily drove survival predictions.

For the MSB-CWXGB configuration—which achieved the highest predictive accuracy—three modalities emerged as the dominant predictors (Figure 5): basic clinical (Source A), medical biology (Source B), and PD-L1 Expression (Source E). These three sources consistently exhibited the highest permutation importance across cross-validation folds.

In addition, the missing-block indicators showed negligible direct contribution to the model (Table 3), indicating that MSB relies on biomarker values rather than on patterns of data availability. While missingness does indirectly influence the model through imputation (e.g., neighbor selection in kNN, pooling of available risk scores), the low permutation importance demonstrates that knowing which blocks are missing added minimal prognostic information beyond what the observed features already provided. This result alleviates two major concerns. First, it suggests that MSB’s predictions were driven by biological signal instead of being confounded by the hospital or protocol from which a patient originated. Second, in corroboration with the KM curve differencing APHM for other patients displaying no statistical difference S3, the site-specific missingness of Source D (vasculo-monitoring), which was only collected at the coordinating center (APHM, accounting for 45% of the cohort) was a concern on potential prognostic bias of missingness. The near-zero importance of these missingness indicators shows that MSB is not merely distinguishing “APHM patients” from “other-center patients,” but instead derives predictive information from the biomarker measurements themselves when they are present. This property is essential for ensuring that the framework remains applicable to other multicenter contexts where different data sources may be unevenly available across sites.

The sparsity of importance across the remaining modalities was largely attributable to the intrinsic feature selection mechanism of component-wise boosting. By updating only one feature at each iteration, CWXGB efficiently identified the most parsimonious set of predictors. For the MSB-CWXGB (or MSB-CWXGB_{imp} variant), if the meta-learner selected the CoxNet score from Source A, the redundant information contained in the RSF or CWXGB scores from the same source is ignored. This leads to a “winner-takes-all” effect at the modality level, where the most informative base-learner for a given source captured the majority of the importance weight (Figure 5).

This pattern of modality dominance remained consistent regardless of the meta-learner architecture, though the distribution of importance varied. CoxNet as meta-learner exhibited a similar sparse profile to component-wise boosting, reinforcing the finding that Sources A, B, and E carry the primary signal for progression-free survival (Figure S5). For RSF as meta-learner, importance scores were more evenly distributed across the modalities. Unlike component wise boosting, RSF does not perform implicit feature selection in the same manner, leading it to leverage a broader combination of base-learner scores (Figure S7).

Despite the inherent variability across data splits, the consistent selection of clinical, biological, and PD-L1 markers underscores the robustness of these features. The relative lack of importance assigned to tumor-based modalities

(Sources F, G, and H) suggests that their predictive signal may either be redundant with more accessible markers or potentially obscured by the high rate of blockwise missingness in those specific sources. Importantly, the negligible importance assigned to the missingness indicators hints that the PIONeER dataset does not suffer from informative missingness bias. This confirms that the absence of a modality—such as tumor-based markers—does not serve as a proxy for patient prognosis. While the model prioritizes clinical and blood markers, it does so based on their substantive predictive value rather than a logistical bias against modalities with higher missingness rates. This finding suggests that MSB effectively isolates physiological signals from the structural patterns of data collection, ensuring that the risk scores are driven by patient biology rather than the presence or absence of specific clinical procedures.

4 Discussion

In this study, we introduced Multimodality Stacking with Blockwise Missing Values (MSB), a novel meta-learning framework designed to address two critical challenges in clinical survival analysis: blockwise missing data and high-dimensional heterogeneity. These challenges are particularly pronounced in multi-center clinical studies, such as the PIONeER dataset, where 39% of data were missing due to heterogeneous data collection protocols across sites [4]. The high-dimensional nature of such datasets—comprising diverse features (e.g., clinical records, biomarkers, imaging)—further complicates analysis, often leading to overfitting and reduced model interpretability [27].

MSB demonstrated performance gains compared with all baseline algorithms (15.9% for linear models, 5.4% for forests, 2.1% for boosting), demonstrating that modality-level decomposition provides greatest value when base learners struggle with high-dimensional heterogeneity. Critically, even state-of-the-art component-wise boosting [7] — which already incorporates implicit feature selection — benefited from MSB’s hierarchical structure (ΔC -index = +0.014, $p=0.030$), suggesting the architectural advantage persists beyond what regularization alone achieves. The substantial reduction in overfitting (train-test gap: 0.055 vs 0.380 for linear models) indicates MSB functions as an effective regularizer, constraining model complexity without sacrificing discriminative power.

The three MSB variants (MSB_{imp}, MSB, MSB_{MIA}) produced comparable results. In a clinical context, this improved calibration implies that the model’s predicted survival probabilities are more aligned with observed outcomes, a prerequisite for using such tools in shared decision-making. Our findings suggest that modality-level aggregation effectively filters intra-source noise, providing a more stable input space for the meta-learner compared to traditional concatenation.

From a clinical implementation perspective, MSB addresses a practical challenge in multi-center oncology trials where specific modalities, such as invasive biopsies, may be unavailable for a subset of the cohort. Conventional multimodal models rely on listwise deletion or computationally intensive imputation,

both of which reduce effective sample size or introduce artifacts. MSB’s source-level aggregation allows predictions despite missing modalities. Imputation is done on a smaller set of features ensuring the framework remains functional across heterogeneous data availability patterns — a critical property for real-world deployment where tissue samples, advanced immune profiling, or genomic sequencing may be selectively collected.

The dominance of readily available markers (clinical features, PD-L1, routine lab biomarkers) over tissue-derived TME profiling carries methodological implications. The weighting of PD-L1 (Source E) aligned with its established role as a biomarker for immunotherapy efficacy in NSCLC [5], while the importance of clinical features and medical biology (Sources A & B) reflected the impact of physiological status and tumor burden on survival outcomes. MSB’s reliance on Sources A, B, and E is consistent with their established clinical role.

On the other hand, despite the established biological relevance of immunohistochemistry based tumor microenvironment (TME) profiling (Sources F, G, and H) contributed marginally.

The marginal contribution of tumor microenvironment modalities likely reflects a combination of methodological constraints and genuine biological redundancy. Among the methodological constraints, Source H’s limited sample size ($n=70$) restricts the meta-learner’s capacity to estimate stable modality-specific weights. Source F’s intrinsically sparse mutation data likely yields near-constant risk scores across patients, causing permutation importance to swap equivalent values and systematically underestimate its true prognostic contribution. Additionally, the winner-takes-all feature selection inherent to component-wise boosting concentrates importance on the single most informative base-learner per modality, suppressing the apparent contribution of correlated sources. Beyond these methodological artifacts, genuine biological redundancy likely accounts for Source G’s modest importance: when PD-L1 expression (Source E) and routine inflammatory markers (Source B) are jointly available, they appear to capture the majority of the prognostic signal contained in broader tumor microenvironment profiling.

MSB builds upon established multimodal learning principles by addressing the specific structural constraints of clinical survival data. While late fusion is well-documented in classification and regression tasks [22], its application to deal with blockwise missingness on such tasks or in survival analysis remains under-explored. Van Loon et al. [22] proposed StaPLR, an imputation-based approach for handling missing modalities in classification tasks using logistic regression. MSB extends this paradigm beyond linear models to survival analysis, where we observed that non-linear methods (RSF, CWXGB) substantially outperformed linear baselines (Table 1). To our knowledge, HEALNet [17] is the only prior work addressing both blockwise missingness and survival learning simultaneously. HEALNet — Hybrid Early-fusion Attention Learning Network — employs a cross-modal attention mechanism to dynamically weight and fuse available modalities, learning a discrete hazard function over binned survival intervals. First, deep learning architectures require substantially larger sample sizes than traditional survival models to avoid overfitting — a chal-

lenge in our cohort with $n=443$, where model complexity must be carefully controlled. Second, HEALNet treats each feature within tabular data as an independent modality, which does not address the high-dimensionality challenge central to our study: the input space remains of dimension $p=378$ regardless of how features are partitioned across modalities. MSB and HEALNet address complementary use cases: HEALNet employs neural architectures to learn cross-modality representations, while MSB uses traditional survival models at the base level and aggregates their outputs. This design is particularly suited to small clinical cohorts, where interpretability and computational efficiency are prioritized. By operating on modality-specific risk scores rather than raw features, MSB reduces the meta-learner input to 24 aggregated predictions ($8 \text{ modalities} \times (3 \text{ base models} + \text{Missingness Rate})$), directly tackling the $n \ll p$ constraint while maintaining interpretability at the source level. Consequently, this framework provides a robust alternative to early fusion for biomarker studies where high dimensionality, blockwise missingness, and data heterogeneity are prevalent.

This study has several limitations, ordered by impact on interpretation and generalizability. First and most critically, all results derived from a single cohort (PIONeeR, $n=443$, 17 French centers), without external validation. While internal cross-validation with statistical testing (Wilcoxon signed-rank tests, FDR correction) demonstrated robust performance, prospective evaluation in independent international cohorts remains essential. External validation should assess whether (1) the 2-16% improvements generalize across populations and standards of care, (2) the dominance of routine clinical and blood markers (Sources A, B, E) persists when TME profiling is more systematically collected, and (3) MSB’s modality-specific importance rankings remain stable across diverse clinical settings. Until externally validated, MSB should be considered a methodological framework for biomarker research rather than a deployment-ready clinical system.

Secondly, this study focused exclusively on PFS as a single endpoint. Clinical oncology frequently involves competing risks (e.g., progression vs. non-cancer death), and extending MSB to competing risk frameworks such as the boosting approach described by Alberge et al. [1] would enable identification of modality-specific predictors tailored to distinct event types, potentially revealing differential biomarker profiles across failure modes. Additionally, the Kaplan-Meier curve (Figure S4) exhibits a plateau after 1000 days, suggesting a subset of patients may experience durable treatment benefit consistent with long-term response. Cure fraction models, which explicitly account for a cured subpopulation, represent an active area of methodological development in survival machine learning [33]. Adapting MSB to incorporate cure fraction estimation — either through mixture cure models at the base learner level or through cure-aware meta-learning — could improve prediction for immunotherapy responders, where long-term remission rates of 20-30% are clinically established [5, 13]. Such extensions would enhance MSB’s ability to distinguish transient response from durable benefit, a critical distinction for treatment planning in immuno-oncology

Finally, while kNN imputation proved effective and computationally efficient, alternative imputation strategies might further enhance predictive fidelity. However, preliminary explorations indicated that implementing more complex imputer in high-dimensional settings ($n \approx p$) requires regularized or tree-based imputation models (e.g., Lasso-based MICE [9], MissForest imputation [28]) to handle multicollinearity, significantly escalating computational costs while risking over-smoothing the data [9]. Given the minimal performance differences between MSB imputation variants (ΔC -index < 0.01 , Table 1), the current kNN approach represented a pragmatic balance between statistical stability and computational tractability. To further address the issue of fine-tuning beyond imputation, we chose to rely on the default hyperparameters for all algorithms, both base and meta estimators, which leaves potential for performance improvement.

5 Conclusion

This study introduced MSB, a novel late-fusion stacking framework designed for multimodal survival analysis in high-dimensional datasets with block-wise missingness. By aggregating modality-specific predictions into a reduced risk-score space, MSB maintained robust predictive performance and cohort size without extensive cross-modality imputation. Validation on the PIONeeR dataset demonstrated MSB’s ability to effectively identify the prognostic importance of clinical, biological, and PD-L1 markers, offering a methodologically sound framework for biomarker evaluation in multicenter oncology studies with heterogeneous data availability. While challenges remain in integrating site-specific modalities due to structural sparsity, MSB’s modular architecture provides a stable and scalable methodology for biomarker discovery and survival prediction in clinical research.

6 Funding Statement

This project has received funding from the Excellence Initiative of Aix-Marseille Université - AMidex, a French “Investissements d’Avenir programme” AMX-21-IET-017.

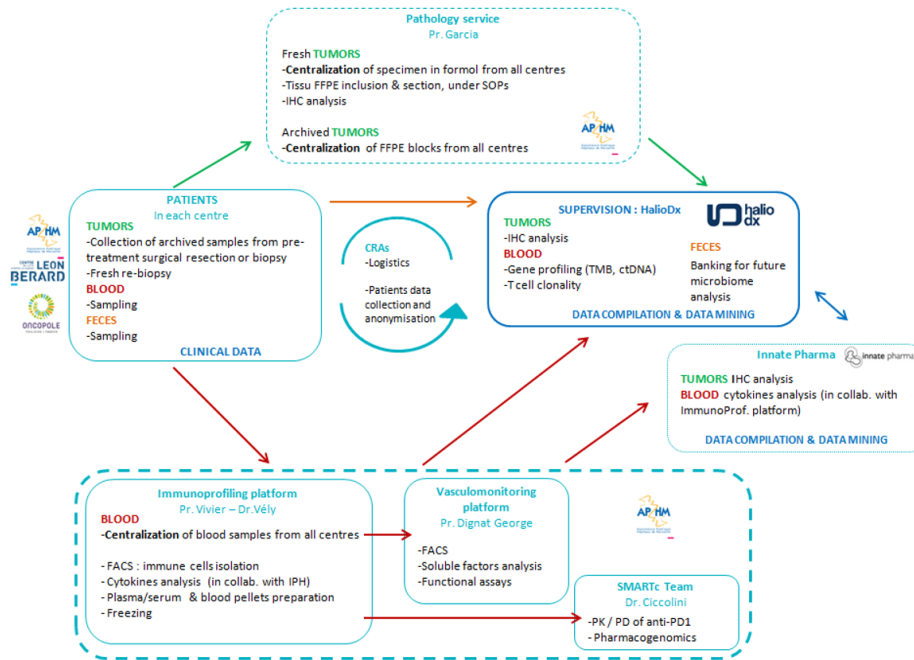
This PIONeeR RHU was funded by a partnership of Aix-Marseille Université (AMU), Assistance Publique Hôpitaux de Marseille (APHM), Centre National de La Recherche Scientifique (CNRS), Institut National de la Santé et de la Recherche Médicale (INSERM), Centre Léon Bérard (CLB), Institut Paoli Calmettes (IPC), Gustave Roussy (GR), AstraZeneca (AZ), Veracyte (VERA), Innate Pharma (IPH) & ImCheck Therapeutics (ICT), and initiated by Marseille Immunopole.

7 Acknowledgment

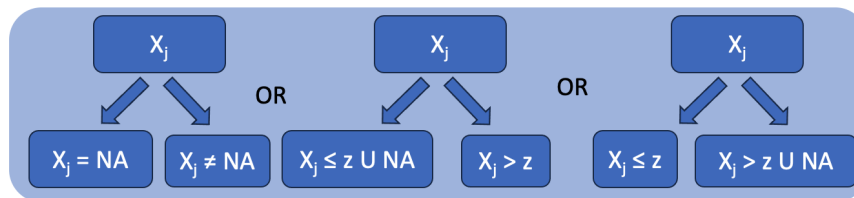
We are grateful to Julie Josse for her invaluable guidance on both the methodological framework and the manuscript's structure. Her insights significantly refined the final paper.

Implementation of the MSB framework is available here under Inria license.

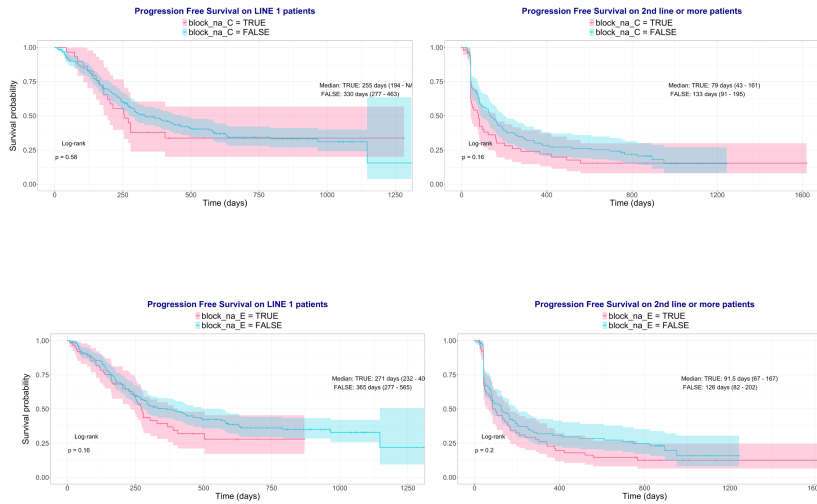
Appendix



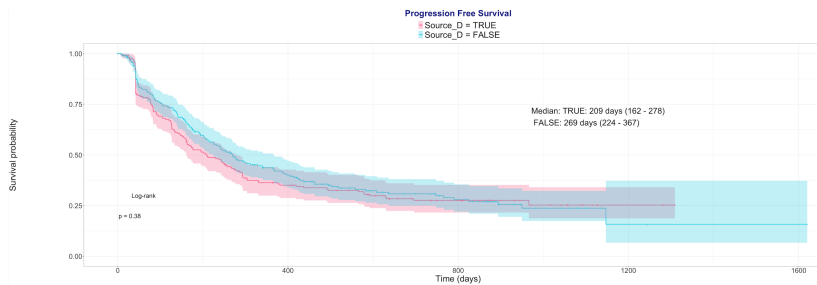
Supplementary Figure S1: How the dataset is built from the patients to labs. Patients that are part of the study are, for each center, sampled (Tumor and Blood) and described with their clinical biomarkers. The samples are then distributed to each partner responsible of a specific analysis in the study. After this steps, the different analysis results are checked and centralized by Veracyte (formerly HaliuDx) for a data lock, ensuring each partner have the same data (the 'Data Compilation' part of the scheme).



Supplementary Figure S2: Missing in attributes splitting options, for a given split, of a feature j at value z . Given a splitting criterion, missing values are either sided against values that are not missing or on one side of the splitting value.



Supplementary Figure S4: KM plots filtered by LINE of patients on sources C and E. All plots shows no significant survival differences between patients with and without available data.



Supplementary Figure S3: Kaplan-Meier curve of patients grouped according to their originating center. The log-rank test is not significant, indicating no statistically significant difference between the two curves. This suggests that the center of origin does not bias survival.

MSBs' performance on Progression only

Table S4: Model performance on progression-only endpoint across 15 cross-validation folds (5-fold CV \times 3 repetitions). Values shown as mean \pm SD. Bold indicates best test performance within family per metric; * indicates global best test performance.

Model Family	Model	Dataset	C-index	iBS Early	iBS Late
Linear	CoxNet _{imp}	test	0.564 \pm 0.039	0.192 \pm 0.029	0.399 \pm 0.039
		train	0.985 \pm 0.005	0.012 \pm 0.003	0.023 \pm 0.004
	MSB-CoxNet _{imp}	test	0.652 \pm 0.043	0.091 \pm 0.013	0.237 \pm 0.040
		train	0.878 \pm 0.057	0.065 \pm 0.009	0.122 \pm 0.033
	MSB-CoxNet	test	0.661 \pm 0.036	0.088 \pm 0.011	0.226 \pm 0.028
		train	0.830 \pm 0.073	0.068 \pm 0.009	0.142 \pm 0.032
Forest	RSF _{imp}	test	0.630 \pm 0.047	0.087 \pm 0.013	0.229 \pm 0.023
		train	0.947 \pm 0.003	0.033 \pm 0.002	0.054 \pm 0.001
	MSB-RSF	test	0.654 \pm 0.033	0.086 \pm 0.011	0.218 \pm 0.022
		train	0.848 \pm 0.019	0.062 \pm 0.002	0.153 \pm 0.012
	MSB-RSF _{imp}	test	0.660 \pm 0.040	0.085 \pm 0.011	0.223 \pm 0.029
		train	0.863 \pm 0.018	0.059 \pm 0.004	0.149 \pm 0.015
	MSB-RSF _{MIA}	test	0.661 \pm 0.034	0.084 \pm 0.010*	0.221 \pm 0.021
		train	0.837 \pm 0.013	0.061 \pm 0.003	0.150 \pm 0.009
Boosting	MSB-XGB _{imp}	test	0.637 \pm 0.044	0.093 \pm 0.018	0.245 \pm 0.031
		train	0.780 \pm 0.092	0.076 \pm 0.014	0.170 \pm 0.033
	MSB-XGB	test	0.640 \pm 0.028	0.092 \pm 0.013	0.236 \pm 0.027
		train	0.787 \pm 0.032	0.077 \pm 0.005	0.165 \pm 0.011
	XGB _{imp}	test	0.651 \pm 0.044	0.087 \pm 0.015	0.248 \pm 0.037
		train	0.954 \pm 0.004	0.041 \pm 0.002	0.070 \pm 0.003
	CWXGB _{imp}	test	0.663 \pm 0.045	0.089 \pm 0.013	0.221 \pm 0.023
		train	0.742 \pm 0.009	0.085 \pm 0.003	0.195 \pm 0.005
	MSB-CWXGB _{imp}	test	0.678 \pm 0.045	0.087 \pm 0.012	0.214 \pm 0.027
		train	0.731 \pm 0.030	0.084 \pm 0.005	0.189 \pm 0.010
	MSB-CWXGB	test	0.687 \pm 0.037*	0.087 \pm 0.011	0.209 \pm 0.018*
		train	0.727 \pm 0.016	0.084 \pm 0.003	0.190 \pm 0.006
Stacking	ScikitsurvStack	test	0.577 \pm 0.043	0.150 \pm 0.023	0.342 \pm 0.050
		train	0.965 \pm 0.008	0.028 \pm 0.003	0.052 \pm 0.005

MSBs’ performance on Death (or Overall Survival)

Table S5: Model Performance on Overall Survival (OS) on PIONeeR dataset across 15 cross-validation folds (5-fold CV \times 3 repetitions). Values shown as mean \pm SD. Bold indicates best test performance within family per metric; * indicates global best test performance. All MSB models include missing block indicators. CWXGB = Component-Wise Gradient Boosting, RSF = Random Survival Forest, XGB = Gradient Boosting, MSB = Multimodality Stacking with Blockwise missing values model.

Model Family	Model	Dataset	C-index	iBS Early	iBS Late
	Random	test	0.500 \pm 0.000	0.250 \pm 0.004	0.251 \pm 0.008
		train	0.500 \pm 0.000	0.250 \pm 0.000	0.250 \pm 0.000
Forest	RSF	test	0.646 \pm 0.040	0.066 \pm 0.020	0.209 \pm 0.011
		train	0.943 \pm 0.002	0.033 \pm 0.002	0.056 \pm 0.001
	RSF _{MIA}	test	0.648 \pm 0.035	0.069 \pm 0.019	0.207 \pm 0.010
		train	0.924 \pm 0.004	0.040 \pm 0.002	0.087 \pm 0.002
	MSB-RSF _{imp}	test	0.675 \pm 0.026	0.068 \pm 0.017	0.203 \pm 0.011
		train	0.863 \pm 0.018	0.052 \pm 0.003	0.135 \pm 0.014
	MSB-RSF _{MIA}	test	0.669 \pm 0.024	0.068 \pm 0.017	0.203 \pm 0.014
		train	0.873 \pm 0.013	0.051 \pm 0.004	0.118 \pm 0.011
	MSB-RSF	test	0.676 \pm 0.025	0.067 \pm 0.017	0.205 \pm 0.015
		train	0.878 \pm 0.015	0.050 \pm 0.003	0.117 \pm 0.010
Boosting	SurvXGB	test	0.649 \pm 0.019	0.069 \pm 0.021	0.225 \pm 0.017
		train	0.934 \pm 0.007	0.034 \pm 0.003	0.076 \pm 0.004
	MSB-XGB _{imp}	test	0.668 \pm 0.020	0.071 \pm 0.018	0.221 \pm 0.019
		train	0.823 \pm 0.033	0.058 \pm 0.005	0.149 \pm 0.028
	MSB-XGB	test	0.670 \pm 0.032	0.071 \pm 0.020	0.222 \pm 0.022
		train	0.842 \pm 0.031	0.057 \pm 0.006	0.133 \pm 0.019
	CWSurvXGB	test	0.658 \pm 0.024	0.067 \pm 0.020	0.204 \pm 0.012
		train	0.739 \pm 0.008	0.063 \pm 0.004	0.179 \pm 0.002
	MSB-CWXGB _{imp}	test	0.674 \pm 0.027	0.066 \pm 0.019	0.204 \pm 0.012
		train	0.868 \pm 0.056	0.051 \pm 0.007	0.122 \pm 0.025
	MSB-CWXGB	test	0.684 \pm 0.020*	0.065 \pm 0.018*	0.199 \pm 0.015*
		train	0.864 \pm 0.045	0.052 \pm 0.006	0.127 \pm 0.022
Stacking	ScikitSurvStack	test	0.653 \pm 0.033	0.067 \pm 0.021	0.229 \pm 0.021
		train	0.935 \pm 0.004	0.040 \pm 0.002	0.075 \pm 0.002

Hyperparameters for results

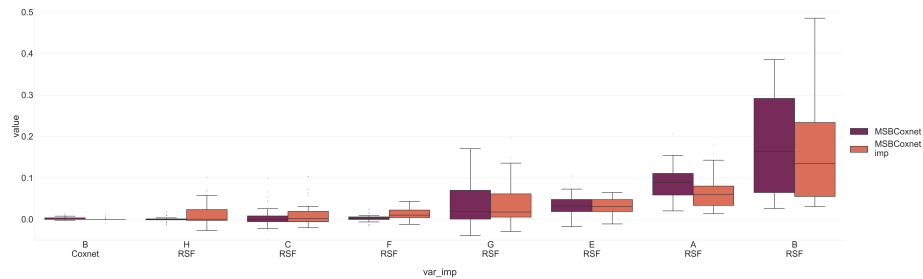
Each Meta learners used in MSB (Coxnet, RSF, CWXGB, XGB) uses default parameters from scikit survival’s API.

For MSB, the stacking procedure uses 5 folds cross validation. the base

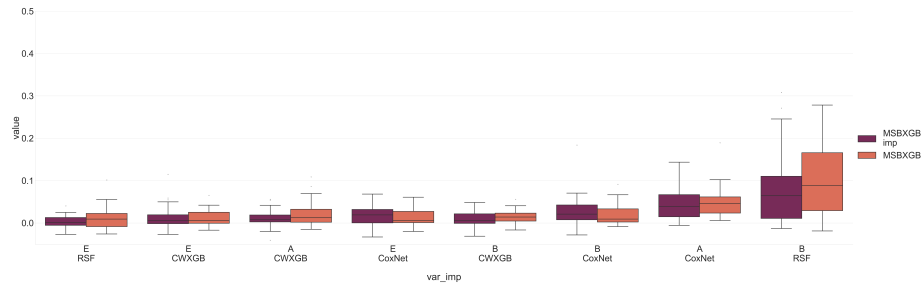
learners are used with default hyperparameters as well as the meta-learner.

On MSB on Overall Survival, the model used a Random Survival Forest with default parameter and Component wise boosting algorithm with $n_estimators = 300$ as hyperparameter, the CoxNet model was removed

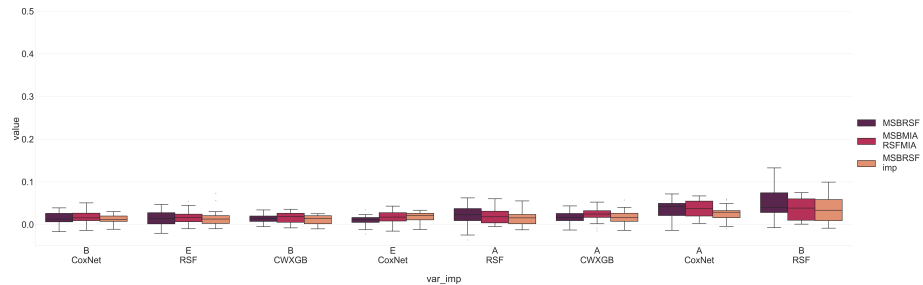
Modality importances for other MSB models



Supplementary Figure S5: Permutation importance on iBSS for CoxNet as meta model for MSB.



Supplementary Figure S6: Permutation importance on iBSS for Gradient boosting as meta model for MSB



Supplementary Figure S7: Permutation importance on iBSS for RSF as meta model in MSB

References

- [1] J. Alberge et al. “P52 - Survival models: Proper scoring rule and stochastic optimization with competing risks”. In: *Journal of Epidemiology and Population Health*. EPICLIN 2025, 19ème Conférence francophone d’Épidémiologie Clinique et 32èmes Journées des Statisticiens des Centres de Lutte Contre le Cancer, Bordeaux, France, 14-16 mai 2025 73 (May 1, 2025), p. 203083. ISSN: 2950-4333. DOI: 10.1016/j.jep.h.2025.203083. URL: <https://www.sciencedirect.com/science/article/pii/S2950433325002770>.
- [2] André Altmann et al. “Permutation importance: a corrected feature importance measure”. In: *Bioinformatics* 26.10 (Apr. 2010), pp. 1340–1347. ISSN: 1367-4803. DOI: 10.1093/bioinformatics/btq134. eprint: https://academic.oup.com/bioinformatics/article-pdf/26/10/1340/48851160/bioinformatics_26_10_1340.pdf. URL: <https://doi.org/10.1093/bioinformatics/btq134>.
- [3] Anastasiia Bakhmach et al. *ROOFS: RObust biOmarker Feature Selection*. 2026. arXiv: 2601.05151 [stat.ML]. URL: <https://arxiv.org/abs/2601.05151>.
- [4] Fabrice Barlesi et al. *An integrative multimodal machine learning signature of primary resistance to immunotherapy in advanced non-small cell lung cancer: biomarker analysis from the PIONeeR study*. ISSN: 3067-2007 Pages: 2026.01.09.26343779. Jan. 11, 2026. DOI: 10.64898/2026.01.09.26343779. URL: <https://www.medrxiv.org/content/10.64898/2026.01.09.26343779v1> (visited on 01/28/2026).
- [5] Hossein Borghaei et al. “Five-Year Outcomes From the Randomized, Phase III Trials CheckMate 017 and 057: Nivolumab Versus Docetaxel in Previously Treated Non-Small-Cell Lung Cancer”. In: *Journal of Clinical Oncology: Official Journal of the American Society of Clinical Oncology* 39.7 (Mar. 1, 2021), pp. 723–733. ISSN: 1527-7755. DOI: 10.1200/JCO.20.01605.
- [6] Freddie Bray et al. “Global cancer statistics 2022: GLOBOCAN estimates of incidence and mortality worldwide for 36 cancers in 185 countries”. In: *CA: a cancer journal for clinicians* 74.3 (2024), pp. 229–263. ISSN: 1542-4863. DOI: 10.3322/caac.21834.
- [7] Peter Bühlmann. “Boosting for high-dimensional linear models”. In: *The Annals of Statistics* 34.2 (2006), pp. 559–583. DOI: 10.1214/009053606000000092. URL: <https://doi.org/10.1214/009053606000000092>.
- [8] Lars Buitinck et al. “API design for machine learning software: experiences from the scikit-learn project”. In: *ECML PKDD Workshop*. 2013, pp. 108–122.
- [9] S. van Buuren. *Flexible Imputation of Missing Data. Second Edition*. Boca Raton, FL.: CRC Press, 2018.

- [10] Nicolas Captier et al. “Integration of clinical, pathological, radiological, and transcriptomic data improves prediction for first-line immunotherapy outcome in metastatic non-small cell lung cancer”. In: *Nature Communications* 16.1 (Jan. 12, 2025), p. 614. ISSN: 2041-1723. DOI: 10.1038/s41467-025-55847-5. URL: <https://www.nature.com/articles/s41467-025-55847-5>.
- [11] E. A. Eisenhauer et al. “New response evaluation criteria in solid tumours: Revised RECIST guideline (version 1.1)”. In: *European Journal of Cancer* 45.2 (Jan. 1, 2009). Publisher: Elsevier, pp. 228–247. ISSN: 0959-8049, 1879-0852. DOI: 10.1016/j.ejca.2008.10.026. URL: [https://www.ejccancer.com/article/S0959-8049\(08\)00873-3/abstract](https://www.ejccancer.com/article/S0959-8049(08)00873-3/abstract).
- [12] Leena Gandhi et al. “Pembrolizumab plus Chemotherapy in Metastatic Non-Small-Cell Lung Cancer”. In: *New England Journal of Medicine* 378.22 (May 31, 2018). Publisher: Massachusetts Medical Society, pp. 2078–2092. ISSN: 0028-4793. DOI: 10.1056/NEJMoa1801005. URL: <https://www.nejm.org/doi/full/10.1056/NEJMoa1801005>.
- [13] Marina C. Garassino et al. “Pembrolizumab Plus Pemetrexed and Platinum in Nonsquamous Non-Small-Cell Lung Cancer: 5-Year Outcomes From the Phase 3 KEYNOTE-189 Study”. In: *Journal of Clinical Oncology: Official Journal of the American Society of Clinical Oncology* 41.11 (Apr. 10, 2023), pp. 1992–1998. ISSN: 1527-7755. DOI: 10.1200/JCO.22.01989.
- [14] Mehmet Gönen and Ethem Alpaydin. “Multiple Kernel Learning Algorithms”. In: *Journal of Machine Learning Research* 12.64 (2011), pp. 2211–2268. ISSN: 1533-7928. URL: <http://jmlr.org/papers/v12/gonen11a.html>.
- [15] Erika Graf et al. “Assessment and comparison of prognostic classification schemes for survival data”. In: *Statistics in Medicine* 18.17 (1999), pp. 2529–2545. ISSN: 1097-0258. DOI: 10.1002/(SICI)1097-0258(19990915/30)18:17<2529::AID-SIM274>3.0.CO;2-5. URL: <https://onlinelibrary.wiley.com/doi/abs/10.1002/%28SICI%291097-0258%2819990915/30%2918%3A17/18%3C2529%3A%3AAID-SIM274%3E3.0.CO%3B2-5>.
- [16] F. E. Harrell, K. L. Lee, and D. B. Mark. “Multivariable prognostic models: issues in developing models, evaluating assumptions and adequacy, and measuring and reducing errors”. In: *Statistics in Medicine* 15.4 (Feb. 28, 1996), pp. 361–387. ISSN: 0277-6715. DOI: 10.1002/(SICI)1097-0258(19960229)15:4<361::AID-SIM168>3.0.CO;2-4.
- [17] Konstantin Hemker, Nikola Simidjievski, and Mateja Jamnik. “HEALNet: Multimodal Fusion for Heterogeneous Biomedical Data”. In: *Advances in Neural Information Processing Systems* 37 (Dec. 16, 2024), pp. 64479–64498. URL: https://proceedings.neurips.cc/paper_files/paper/2024/hash/765871e77d2ca65126d3d64d31aa6908-Abstract-Conference.html.

- [18] Julie Josse et al. “On the consistency of supervised learning with missing values”. In: *Statistical Papers* 65.9 (Dec. 1, 2024), pp. 5447–5479. ISSN: 1613-9798. DOI: 10.1007/s00362-024-01550-4. URL: <https://doi.org/10.1007/s00362-024-01550-4>.
- [19] J. Keyl et al. “Multimodal survival prediction in advanced pancreatic cancer using machine learning”. In: *ESMO Open* 7.5 (Aug. 18, 2022), p. 100555. ISSN: 2059-7029. DOI: 10.1016/j.esmoop.2022.100555. URL: <https://pmc.ncbi.nlm.nih.gov/articles/PMC9588888/>.
- [20] Felix Krones et al. “Review of multimodal machine learning approaches in healthcare”. In: *Information Fusion* 114 (Feb. 1, 2025), p. 102690. ISSN: 1566-2535. DOI: 10.1016/j.inffus.2024.102690. URL: <https://www.sciencedirect.com/science/article/pii/S1566253524004688>.
- [21] Mark J. van der Laan, Eric C. Polley, and Alan E. Hubbard. “Super learner”. In: *Statistical Applications in Genetics and Molecular Biology* 6 (2007), Article25. ISSN: 1544-6115. DOI: 10.2202/1544-6115.1309.
- [22] Wouter van Loon et al. “Imputation of missing values in multi-view data”. In: *Information Fusion* 111 (Nov. 1, 2024), p. 102524. ISSN: 1566-2535. DOI: 10.1016/j.inffus.2024.102524. URL: <https://www.sciencedirect.com/science/article/pii/S1566253524003026>.
- [23] Steven Nowlan and Geoffrey E Hinton. “Evaluation of Adaptive Mixtures of Competing Experts”. In: *Advances in Neural Information Processing Systems*. Ed. by R.P. Lippmann, J. Moody, and D. Touretzky. Vol. 3. Morgan-Kaufmann, 1990. URL: https://proceedings.neurips.cc/paper_files/paper/1990/file/432aca3a1e345e339f35a30c8f65edce-Paper.pdf.
- [24] Alexandre Perez-Lebel et al. “Benchmarking missing-values approaches for predictive models on health databases”. In: *GigaScience* 11 (Apr. 2022), giac013. ISSN: 2047-217X. DOI: 10.1093/gigascience/giac013. eprint: <https://academic.oup.com/gigascience/article-pdf/doi/10.1093/gigascience/giac013/60706597/giac013.pdf>. URL: <https://doi.org/10.1093/gigascience/giac013>.
- [25] Sebastian Pölsterl. “scikit-survival: A Library for Time-to-Event Analysis Built on Top of scikit-learn”. In: *Journal of Machine Learning Research* 21.212 (2020), pp. 1–6. ISSN: 1533-7928. URL: <http://jmlr.org/papers/v21/20-729.html>.
- [26] Naiyer Rizvi et al. “Society for Immunotherapy of Cancer (SITC) consensus definitions for resistance to combinations of immune checkpoint inhibitors with chemotherapy”. In: *Journal for ImmunoTherapy of Cancer* 11.3 (Mar. 14, 2023). ISSN: 2051-1426. DOI: 10.1136/jitc-2022-005920. URL: <https://jitc.bmj.com/content/11/3/e005920>.

- [27] Stephen Salerno and Yi Li. “High-Dimensional Survival Analysis: Methods and Applications”. In: *Annual review of statistics and its application* 10.1 (Mar. 2023), pp. 25–49. ISSN: 2326-8298. DOI: 10.1146/annurev-statistics-032921-022127. URL: <https://www.ncbi.nlm.nih.gov/pmc/articles/PMC10038209/>.
- [28] Daniel J. Stekhoven and Peter Bühlmann. “MissForest—non-parametric missing value imputation for mixed-type data”. In: *Bioinformatics* 28.1 (Oct. 2011), pp. 112–118. ISSN: 1367-4803. DOI: 10.1093/bioinformatics/btr597. eprint: https://academic.oup.com/bioinformatics/article-pdf/28/1/112/50568519/bioinformatics_28_1_112.pdf. URL: <https://doi.org/10.1093/bioinformatics/btr597>.
- [29] Sandra Steyaert et al. “Multimodal data fusion for cancer biomarker discovery with deep learning”. In: *Nature machine intelligence* 5.4 (Apr. 2023), pp. 351–362. ISSN: 2522-5839. DOI: 10.1038/s42256-023-00633-5. URL: <https://pmc.ncbi.nlm.nih.gov/articles/PMC10484010/>.
- [30] Hussein A. Tawbi et al. “Society for Immunotherapy of Cancer (SITC) checkpoint inhibitor resistance definitions: efforts to harmonize terminology and accelerate immuno-oncology drug development”. In: *Journal for ImmunoTherapy of Cancer* 11.7 (July 24, 2023). ISSN: 2051-1426. DOI: 10.1136/jitc-2023-007309. URL: <https://jitc.bmj.com/content/11/7/e007309>.
- [31] Olga Troyanskaya et al. “Missing value estimation methods for DNA microarrays”. In: *Bioinformatics* 17.6 (June 2001), pp. 520–525. ISSN: 1367-4803. DOI: 10.1093/bioinformatics/17.6.520. eprint: https://academic.oup.com/bioinformatics/article-pdf/17/6/520/48837104/bioinformatics_17_6_520.pdf. URL: <https://doi.org/10.1093/bioinformatics/17.6.520>.
- [32] B.E.T.H. Twala, M.C. Jones, and D.J. Hand. “Good methods for coping with missing data in decision trees”. In: *Pattern Recognition Letters* 29.7 (2008), pp. 950–956. ISSN: 0167-8655. DOI: <https://doi.org/10.1016/j.patrec.2008.01.010>. URL: <https://www.sciencedirect.com/science/article/pii/S0167865508000305>.
- [33] Huina Wang, Tian Feng, and Baosheng Liang. “Improved Mixture Cure Model Using Machine Learning Approaches”. In: *Mathematics* 13.4 (Feb. 8, 2025). Company: Multidisciplinary Digital Publishing Institute Distributor: Multidisciplinary Digital Publishing Institute Institution: Multidisciplinary Digital Publishing Institute Label: Multidisciplinary Digital Publishing Institute. ISSN: 2227-7390. DOI: 10.3390/math13040557. URL: <https://www.mdpi.com/2227-7390/13/4/557>.
- [34] David H. Wolpert. “Stacked generalization”. In: *Neural Networks* 5.2 (Jan. 1, 1992), pp. 241–259. ISSN: 0893-6080. DOI: 10.1016/S0893-6080(05)80023-1. URL: <https://www.sciencedirect.com/science/article/pii/S0893608005800231>.

- [35] Renjie Wu et al. *Deep Multimodal Learning with Missing Modality: A Survey*. Oct. 21, 2024. DOI: 10.48550/arXiv.2409.07825. arXiv: 2409.07825[cs]. URL: <http://arxiv.org/abs/2409.07825>.
- [36] Shuo Xiang et al. “Bi-level Multi-Source Learning for Heterogeneous Block-wise Missing Data”. In: *NeuroImage* 102 Pt 1 (Nov. 15, 2014), pp. 192–206. ISSN: 1053-8119. DOI: 10.1016/j.neuroimage.2013.08.015. URL: <https://www.ncbi.nlm.nih.gov/pmc/articles/PMC3937297/>.
- [37] Chang Xu, Dacheng Tao, and Chao Xu. *A Survey on Multi-view Learning*. 2013. arXiv: 1304.5634 [cs.LG]. URL: <https://arxiv.org/abs/1304.5634>.
- [38] Fei Zhao, Chengcui Zhang, and Baocheng Geng. “Deep Multimodal Data Fusion”. In: *ACM Comput. Surv.* 56.9 (2024), 216:1–216:36. ISSN: 0360-0300. DOI: 10.1145/3649447. URL: <https://dl.acm.org/doi/10.1145/3649447>.